Supporting Information

Gigaton Commercial-Scale Carbon Storage and Mineralization Potential in Stacked Columbia River Basalt Reservoirs

Ruoshi Cao [a]*, Quin R.S. Miller [a]*, Casie L. Davidson [a], William Gallin [b], Stephen P. Reidel [a#], Zunsheng Jiao [c], J. Fred McLaughlin [c], H. Todd Schaef [a]*

[a] Energy and Environment Directorate, Pacific Northwest National Laboratory, Richland, Washington, 99354, USA
[b] Washington Department of Natural Resources, Washington Geological Survey, Olympia, Washington, 98504, USA
[d] Center for Economic Geology Research, University of Wyoming, 1000 E. University Avenue, Laramie, WY, 82071, USA
[#] Retired

*Corresponding Authors
Ruoshi Cao, ross.cao@pnnl.gov
Quin R.S. Miller, quin.miller@pnnl.gov
Todd Schaef, todd.schaef@pnnl.gov

9 Pages
Tables S1-S3
Figures S1-S5

Series		Group	Formation	Member	# of Flows	Age (m.a.)
Miocene	Upper	Columbia River Basalt Group	Saddle Mountains Basalt	Lower Monumental Member		6
				Ice-Harbor Member		8.5
				Buford Member		
				Elephant Mountain Member		10.5
	Middle			Pomona Member		12
				Esquatzel Member		
				Weissenfels Ridge Member		
				Asotin Member		13
				Wilbur Member		
				Umatilla Member		
			Wanapum Basalt	Priest Rapids Member		14.5
				Roza Member		
				Shumaker Creek Member		
				Frenchman Springs Member		15.3
				Eckler Mountain Member		
			Grande Ronde Basalt	Sentinel Bluffs Member	>10	15.6
				Winter Water Member	>4	
				Indian Ridge Member	2 and 1 lobe	
				Armstrong Canyon Member	>4	
				Ortley Member	>7	
	Lower			Buttermilk Canyon Member	2 to 3	
				Grouse Creek Member	>5	
				Wapshilla Ridge Member	>18	
				Mount Horrible Member	>4	
				Cold Spring Ridge Member	1 to 3	
				Hoskin Gulch Member	3 to 6	
				China Creek Member	1 to 3	
				Frye Point Member	1 to 4	
				Downey Gulch Member	5 to 7	
				Center Creek Member	5	
				Skeleton Creek Member	3	
				Rogersburg Member	5	
				Teepee Butte Member	3 to 7	
				Buckhom Springs	6	16.5
			Imnaha Basalt			17.5

Figure S1. Stratigraphic nomenclature of the Columbia River Basalt Group in the study area. Modified after Reidel et al., 2003[1] and Reidel and Tolan., 2013[2].

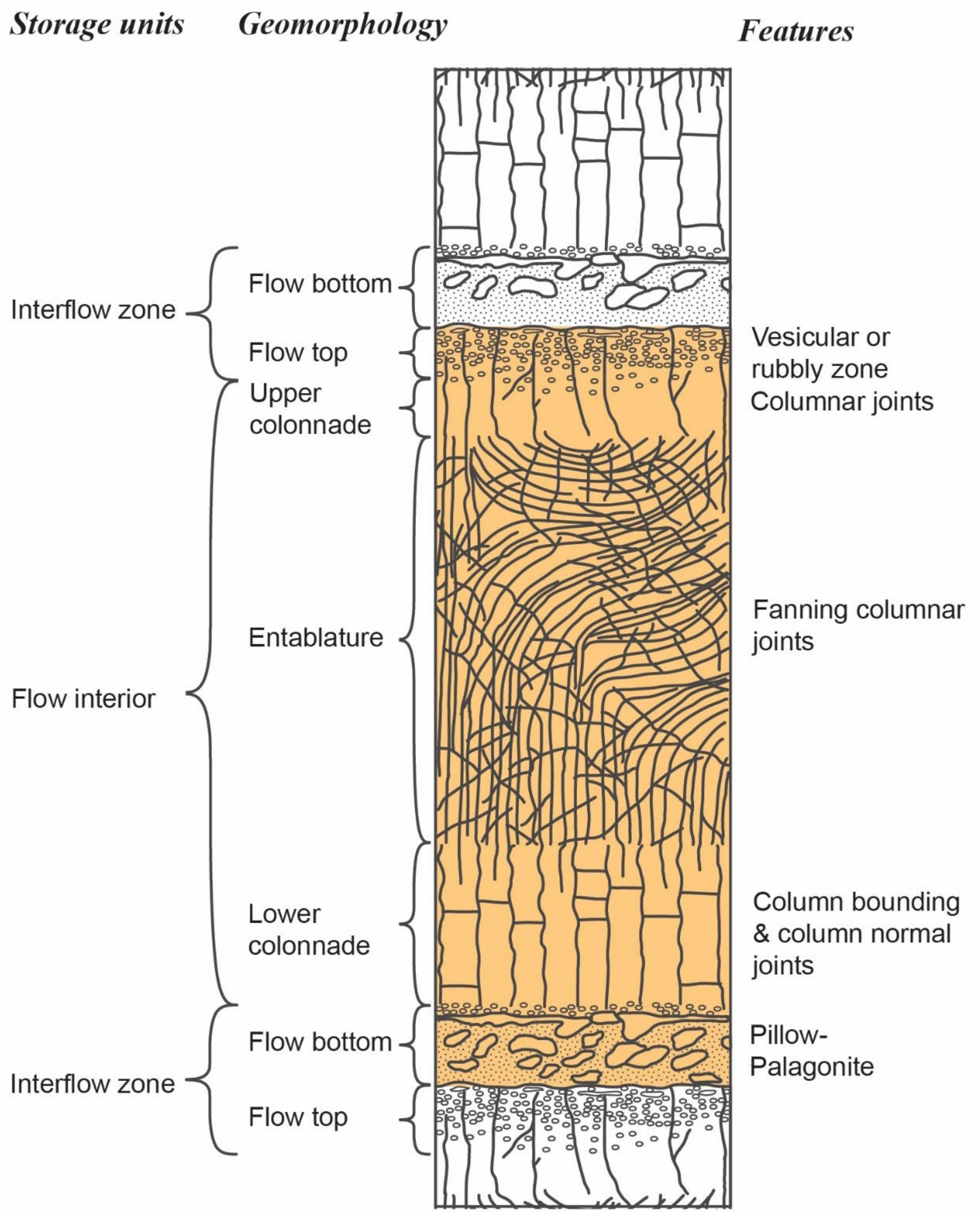

Figure S2. Schematic categorization of internal features of typical stacked lava flows in the Columbia River Basalt Group, modified from Swanson et al. 1979[3], Reidel et al. 2013[4], and Gierzynski and Pollyea, 2017[5]. The color-shaded section is a typical lava flow intercalated between an underlying older flow and an overlying younger flow.

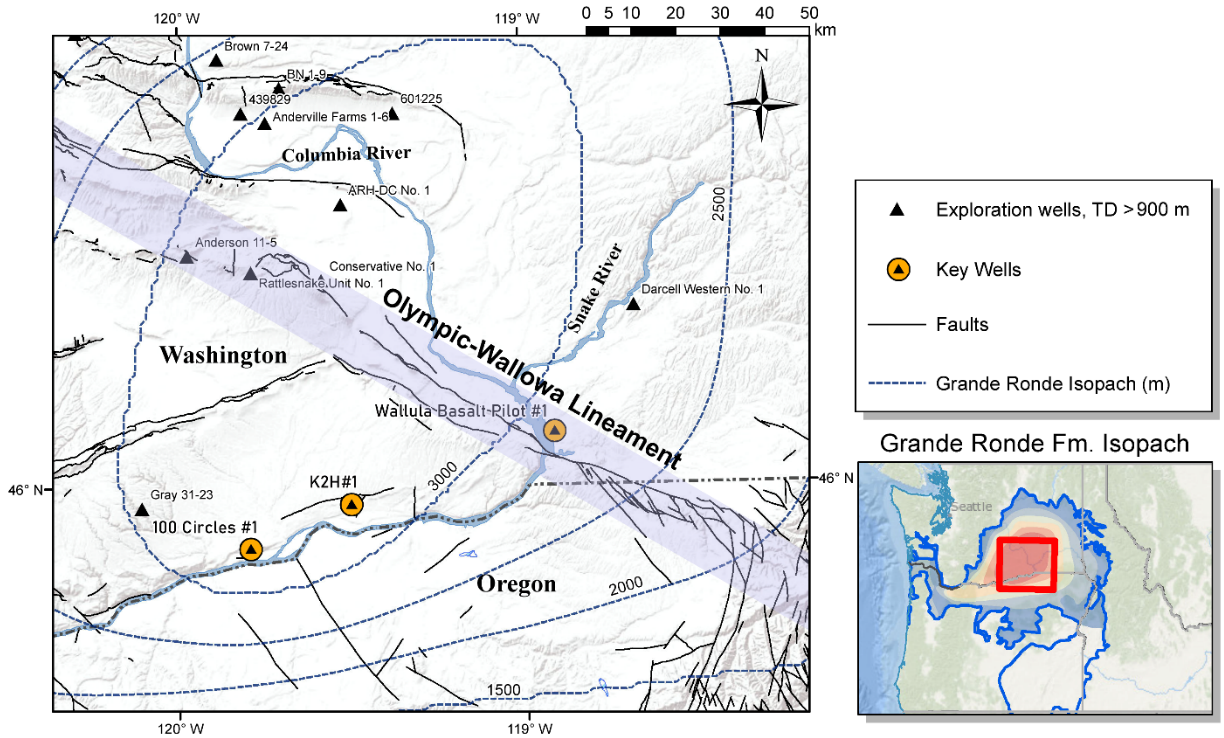

Figure S3. Sub-basinal structure map showing major structure features in the surrounding region, key well locations, deep exploration well locations, and Olympic-Wallowa Lineament (blue-shaded area) in the study area. Refer to the **Figure 2** legend for the inset map.

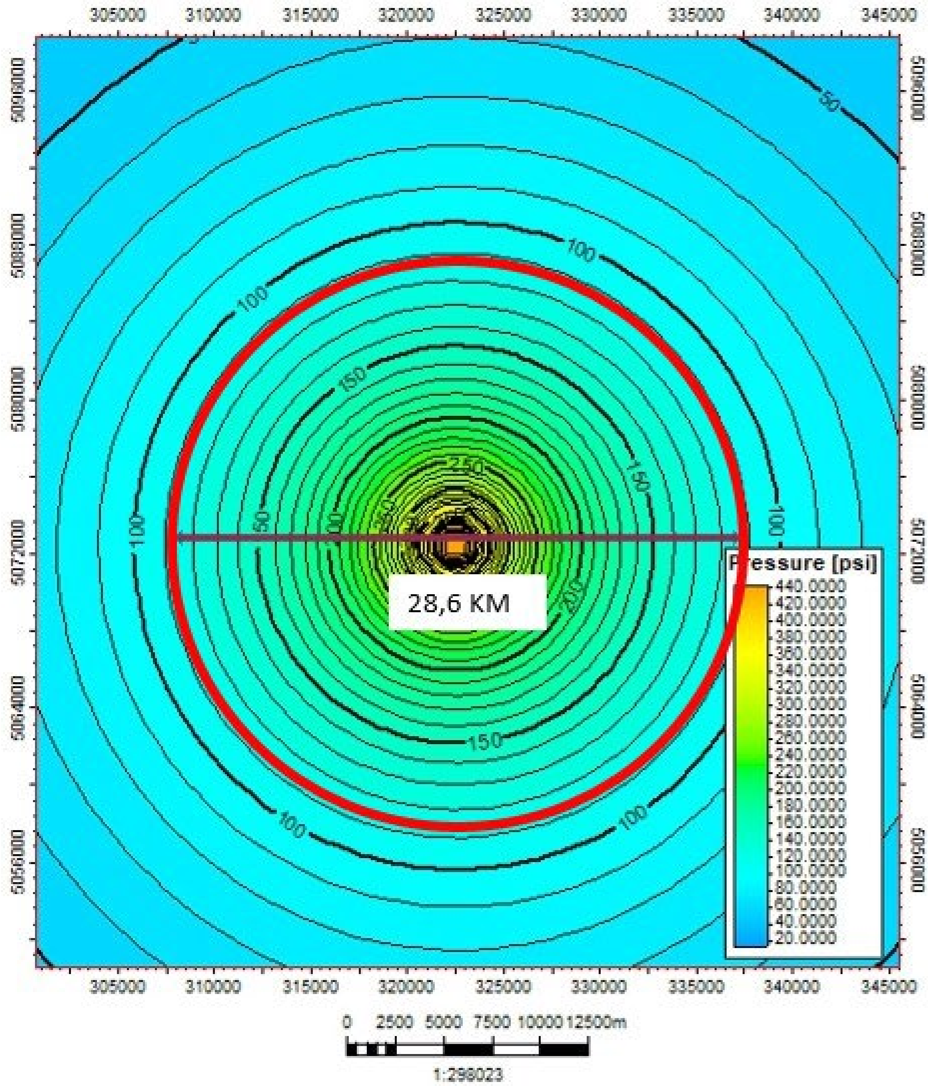

Figure S4. Above figure shows the increase in reservoir pressure (delta pressure) for a CO_2 injection case controlled by the bottom hole pressure. The red circle is the pressure front delineated by Dp contour line of 116 psi.

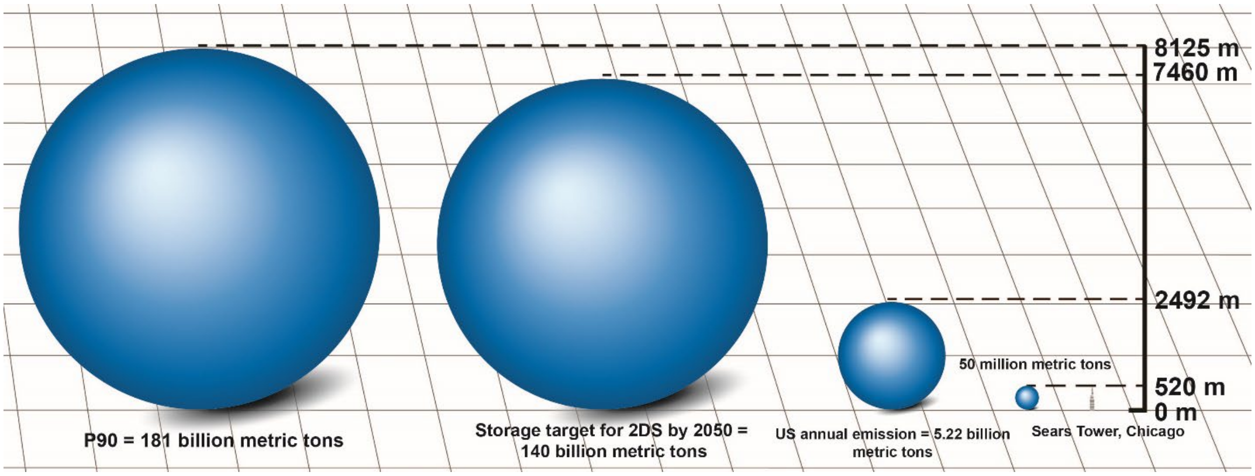

Figure S5. The supercritical CO_2 volumes of (from left to right) P90 resource estimation, average geologic carbon storage target to achieve IEA's 2-degree scenario (2DS)[6], 2020 US annual net CO_2 emission (EPA Facility Level Information on Greenhouse gases Tool), and 50 MMT, in comparison to Sears Tower, Chicago.

Well Name	TD (m)	SP	GR	NPHI	DPHI	Sonic	RHOB	HRLA	T	P	Caliper
Wallula Basalt Pilot #1	1253	✓	✓	✓	✓	✓	✓	✓	✓	✓	✓
K2H #1	1173		✓			✓					
100 Circles #1	1067	✓	✓	✓	✓		✓	✓			✓

Table S1. Well logs from the three key wells used to characterize flow tops and correlate formations in the Area of Interest. TD – total depth below ground, SP – spontaneous potential, GR – gamma ray, NPHI – neutron porosity, DPHI – density porosity, Sonic – acoustic slowness, RHOB – bulk density, HRLA – deep-shallow resistivity, T – borehole temperature, P - borehole pressure, Caliper – borehole diameter.

Interflow Zone	Depth (m)	Thickness (m)	Porosity (%)	Temperature (K)	Pressure (MPa)
W1	802.3	6.3	38.9	305.1	7.87
W2	830.1	16.3	34.6	306.1	8.14
W3	854.2	7.8	20.5	306.8	8.38
W4	866.1	10.5	21.1	307.2	8.50
W5	894.5	7.8	31.5	307.9	8.78
W6	911.8	10.7	22.8	308.4	8.94
W7	926.9	2.9	22.2	308.8	9.09
W8	933.4	4.2	27	309.1	9.16
W9	984.9	4.4	22.5	310.5	9.66
W10	991.7	7.1	23.6	310.6	9.73
W11	1001.3	1.6	15	311.1	9.82
W12	1033.3	8.7	23.2	312.0	10.14
W13	1055.9	4.4	16.9	313.0	10.36
W14	1084.3	8.1	21.4	313.8	10.64
W15	1100.1	13.7	29.5	314.3	10.79
W16	1161.1	8.0	22.8	316.9	11.39
W17	1242.0	7.5	22.9	320.3	12.18

Table S2. Parameters of Wallula interflow zones in **Figure 3**.

Parameters	P10	P50	P90	Unit	Description
A_t	88,000	88,000	88,000	km^2	Geographical area being assessed for CO_2 storage.
h_g	2,200	2,200	2,200	m	Gross thickness of saline formations for which CO_2 storage is assessed within the region defined by A_t.
Φ_{Total}	0.253	0.253	0.253	n/a	Total porosity in volume defined by the net thickness.
ρ	644	644	644	kg/m^3	Density of CO_2 evaluated at pressure and temperature that represents storage conditions anticipated for a specific geologic unit averaged over h_g and A_t.
$E_{An/At}$	0.2	0.2	0.2	n/a	Fraction of total basin or region area with a suitable formation.
$E_{hn/hg}$	0.27	0.27	0.27	n/a	Fraction of total geologic unit that meets minimum porosity and permeability
$E_{\Phi e/\Phi tot}$	0.82	0.76	0.7	n/a	Fraction of total porosity that is effective, i.e., interconnected.
E_V	0.35	0.46	0.41	n/a	Combined fraction of immediate volume surrounding an injection well that can be contacted by CO_2 and fraction of net thickness that is contacted by CO_2 as a consequence of the density difference between CO_2 and in situ water.
E_d	0.72	0.51	0.37	n/a	Fraction of pore space unavailable due to immobile in situ fluids.
G_{CO2}	351,982	303,702	180,879	MMT	Mass estimate (million metric tons; MMT) of saline formation CO_2 storage resource.

Table S3. CO_2 storage resource estimation (in million metric tons) in GRB interflow zones (800 m ~ 3,000 m). Site-specific storage coefficients ($E_{An/At}$, $E_{\Phi e/\Phi tot}$, E_V, and E_d) are approximated from anticlinal sandstone reservoir deposited in alluvial fan environment [7].

References

(1) Reidel, S. P.; Martin, B. S.; Petcovic, H. L. The Columbia River flood basalts and the Yakima fold belt. *Field Guides* **2003**, *4*, 87-105.

(2) Reidel, S. P.; Tolan, T. L. The Grande Ronde Basalt, Columbia River Basalt Group. *Geological Society of America Special Papers* **2013**, *497*, 117-153.

(3) Swanson, D. A.; TL, W.; PR, H.; RD, B. Revisions in stratigraphic nomenclature of the Columbia River Basalt Group. **1979**.

(4) Reidel, S. P.; Camp, V. E.; Tolan, T.; Martin, B. S. The Columbia River Flood Basalt Province: Stratigraphy, Areal Extent, Volume, and Physical Volcanology. *geological society of America special paper* **2013**, *497*, 1-43.

(5) Gierzynski, A. O.; Pollyea, R. M. Three-phase CO_2 flow in a basalt fracture network. *Water Resources Research* **2017**, *53* (11), 8980-8998.

(6) Mac Dowell, N.; Fennell, P. S.; Shah, N.; Maitland, G. C. The role of CO_2 capture and utilization in mitigating climate change. *Nature Climate Change* **2017**, *7* (4), 243-249.

(7) Gorecki, C. D.; Sorensen, J. A.; Bremer, J. M.; Knudsen, D.; Smith, S. A.; Steadman, E. N.; Harju, J. A. Development of storage coefficients for determining the effective CO_2 storage resource in deep saline formations. In *SPE International Conference on CO2 Capture, Storage, and Utilization*, 2009, 2009; OnePetro: Vol. 126444.